Sci. Dril., 35, 193–209, 2026
https://doi.org/10.5194/sd-35-193-2026

Scientific Drilling
Open Access

Science Reports

Where are the lake deposits? Two atypical overdeepening fills from the Rhine Glacier lobe in southwestern Germany

Johannes E. Pomper[1], **Christian Zeeden**[2], **Frank Preusser**[1], **Ulrike Wielandt-Schuster**[3], **and Lukas Gegg**[1]

[1]Institute of Earth and Environmental Sciences, University of Freiburg, 79104 Freiburg, Germany
[2]LIAG Institute for Applied Geophysics, Stilleweg 2, 30655 Hannover, Germany
[3]Regierungspräsidium Freiburg, Landesamt für Geologie, Rohstoffe und Bergbau (LGRB), 79104 Freiburg, Germany

Correspondence: Johannes E. Pomper (johannes.pomper@geologie.uni-freiburg.de)

Received: 10 March 2026 – Revised: 20 June 2026 – Accepted: 9 July 2026 – Published: 29 September 2026

Abstract. During the Pleistocene, the Alpine landscape and its surroundings were repeatedly reshaped by glacial cycles. Subglacial erosion carved out overdeepened basins into bedrock. Their sedimentary fillings are important archives for understanding the glacial impact on environmental transformation and the history of the Alpine region. Some of these infills are composed of multiple cycles representing separate glaciations; in typical cases, each is represented by a succession of lake deposits. While sediments of earlier glaciations are often eroded by subsequent glaciation cycles, these can be preserved in overdeepened troughs. The International Continental Scientific Drilling Program (ICDP) project "Drilling Overdeepened Alpine Valleys" (DOVE) investigates overdeepened structures on a larger scale by recovering sediment cores around the foreland of the European Alps. As part of the DOVE venture, we present two high-quality drill cores highlighting different basin generations from within the former Rhine Glacier domain of Upper Swabia in southern Germany. The first drilling ICDP 5068_6 near the village Gaisbeuren is located in the low-lying central part of the Rhine Glacier area. We subdivided the 144 m long ICDP 5068_6 core into four sedimentological lithotypes that, in seven stratigraphic units, build up the basin infill. The deposits reveal a glacially sheared bedrock horizon with overlying diamict layers, diamictic fines, and massive sands in alternating sequences. The sedimentary deposits show structureless sections attributed to melt-out, as well as presumed glacio-tectonic deformations. At the hamlet of Lichtenegg, a 76 m long core was recovered from a drill site on the Höchsten butte, targeting the correspondent small-scale Lichtenegg basin. Due to the basin's exceptional, elevated stratigraphic position underlying presumed Early Pleistocene (glacio-)fluvial gravel, it was included in the DOVE project as a bonus site. Based on petrographic and lithological features we divided the core contents into six sedimentological lithotypes and five lithostratigraphic units. The lowermost parts of the infill, which overlie the Molasse bedrock, consist of (sub-)glacial diamicts with glaciolacustrine to glaciodeltaic sediments followed by the (glacio-)fluvial gravels, with additional glacial diamicts on top. Therefore, both investigated cores differ strikingly from the above-mentioned, "typical" lacustrine-dominated sediment successions in overdeepened basins, which we attribute to a continuously ice-proximal setting during infilling. This study emphasizes the variability of overdeepening fills depending on the specific location within the basin and relative to the glacier front.

1 Introduction

The research conducted over the past two centuries on Alpine glaciations has revealed that the Alps and their foreland were subject to extensive glaciations during numerous Pleistocene cold stages (Ellwanger et al., 2011; Monegato et al., 2023; Monegato and Ravazzi, 2018; Preusser et al., 2011). A characteristic landform of former and current glaciated regions is overdeepenings (ODs), valleys, and basins sometimes carved several hundred meters deep into existing topography by subglacial erosion (Cook and Swift, 2012; Preusser et al., 2011). Thanks to intense efforts in OD research in the Alpine forelands, combining geophysical exploration and scientific drilling, the understanding of these basins has significantly improved in recent years. The formation of ODs has been linked to the action of pressurized subglacial water that results in complex trough morphologies (Dürst Stucki and Schlunegger, 2013; Gegg et al., 2021; Schlunegger et al., 2024) that have been formed over several consecutive glaciation phases (Bandou et al., 2022, 2023). The earliest phases of OD formation therefore predate the penultimate glaciation (Buechi et al., 2024; Firla et al., 2026; Schwenk et al., 2022a; Tomonaga et al., 2024). Due to their dimensions and stratigraphic reach, the sediment infills of ODs are an important archive for environmental reconstruction of Alpine glaciations (Gegg and Preusser, 2023).

Based on this wealth of information, the International Continental Scientific Drilling Program (ICDP) project "Drilling Overdeepened Alpine Valleys" (DOVE; http://www.dove-icdp.eu, last access: 13 August 2026) investigates these archives in a two-phase pan-Alpine approach (phase I: northern Alps; phase II: southern Alps) by conducting new drillings and integrating legacy cores, as well as existing data (Anselmetti et al., 2022). Previous (e.g., Buechi et al., 2018, 2024; Dehnert et al., 2012; Pomper et al., 2017; Schwenk et al., 2022a, b) and new investigations (Firla et al., 2024, 2026; Schaller et al., 2023, 2025; Schmalfuss et al., 2026; Schuster et al., 2024) show that the sedimentary fillings of ODs in the northern Alpine foreland frequently consist of thin basal diamicts of glacial origin (Buechi et al., 2017), overlain by thick lacustrine to distal–deltaic successions and, finally, fluvial deposits. We consider this lacustrine-dominated facies to be the "typical" case of OD fills (without further distinguishing, for example, fine-grained or sand-dominated composition; see examples below). However, most of the previous drillings in ODs were conducted in (ice-)distal positions, often with little direct impact from the retreating glacier, and it has to be questioned whether their examined infills are representative of ODs in general. This notion is based on observations from modern Alpine lakes, where more complex OD settings occur, containing additional large-scale depositional features and landforms. Examples are well-developed channel-dissected deltas observed in Lake Brienz (Fabbri et al., 2021), as well as the subaqueous moraine complexes of Lake Lucerne (Hilbe et al., 2011) and Lake Thun (Fabbri et al., 2018).

This study focuses on southwestern Germany, i.e., the area north of Lake Constance in Upper Swabia, which is referred to as Lake Constance Amphitheatre and has been shaped by multiple advances of the Rhine Glacier (Fig. 1; Ellwanger et al., 2011). Its piedmont lobe covered this area several times (Ellwanger et al., 2011; Fiebig et al., 2011), leaving behind several generations of vast ODs, including the present lake basin at its center, as well as today's hilly ice decay landscape with prominent moraine ridges and only sporadic outcrops of the Neogene Molasse bedrock (Jong et al., 2025; Kamleitner et al., 2023; LGRB, 2015). The former (i.e., preglacial) ramp-like Alpine foothill area was therefore strongly re-shaped by ice and meltwater (Cohen et al., 2023) during the Pleistocene with, locally, up to ~ 1 km in vertical incision (Ellwanger et al., 2011).

Two major overdeepened basins in the Lake Constance Amphitheatre were recently surveyed within the scope of the ICDP DOVE project (Fig. 1). The Tannwald Basin situated to the north of Lake Constance was investigated based on three drillings at ICDP site 5068_1 (TANN; Schaller et al., 2025; Schuster et al., 2024) plus an extensive reflection- (Burschil et al., 2018) and cross-hole seismic campaign (Beraus et al., 2024, 2025). The Basadingen Trough to the west of Lake Constance was examined by the ICDP drilling 5068_2 (BASA; Schaller et al., 2023, 2025) on Swiss territory. Both OD basins show generally typical but still different sediment successions. TANN displays a basin fill that consists mostly of fine-grained lacustrine deposits (Schuster et al., 2024), whereas BASA shows an overall more coarse-grained, sand-dominated basin infill (Schaller et al., 2023). Because both sites are located in distal positions within the Rhine Glacier area, the question arises as to whether their successions capture the full variability and complexity of OD infill types in the region. In the following, we introduce two new sites from more central, i.e., proximal, positions within the amphitheater. They were each investigated based on cores from scientific drillings reaching > 10 m into the bedrock, in order to guarantee recovery of the entire Quaternary basin infills. While both sites were originally targeted in order to close stratigraphic gaps, they revealed, first of all, unexpected, diamict-dominated sediment fills that are in contrast to the above-mentioned, "typical" lacustrine deposits. Here, we present these "atypical" lithostratigraphic successions of sediments in the GAIS and LICH drill cores, which are complemented by selected borehole and core geophysical data and standard sedimentological analyses, in order to improve our understanding of sediment variability in these basins.

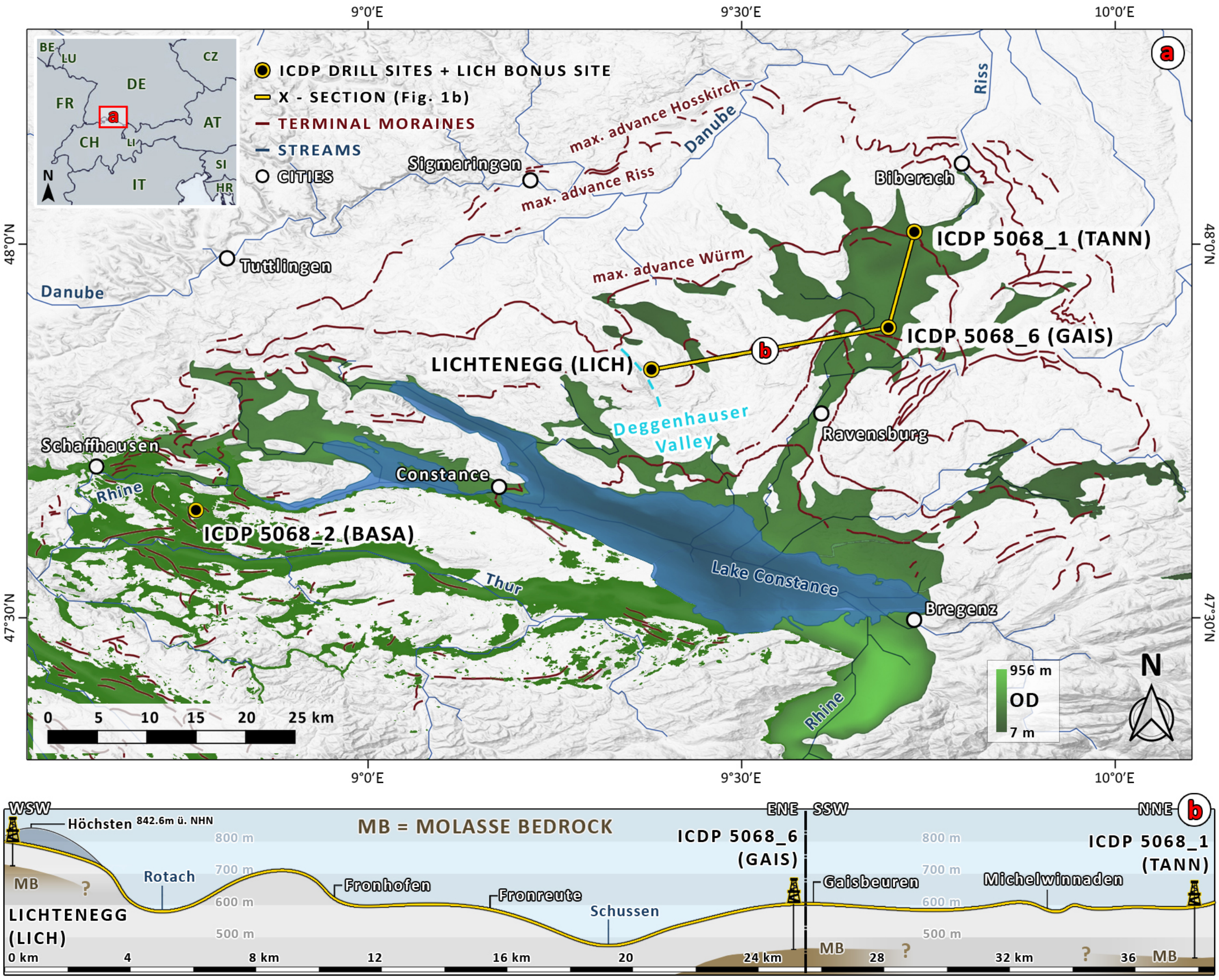

Figure 1. **(a)** Overview of the Quaternary overdeepened structures (green basins; OD denotes overdeepened depth below fluvial base level) below the former Rhine Glacier lobe in the Lake Constance Area in Upper Swabia (modified from Gegg et al., 2025a, and Swisstopo 2025, 2025). Elevation data (TanDEM-X 30 m) are provided by the German Aerospace Centre (DLR). **(b)** Cross-section through drill sites LICH-GAIS-TANN.

2 Study areas

2.1 Gaisbeuren (5068_6)

The first site (5068_6, GAIS) is located near Gaisbeuren, approximately 12 km to the south of TANN (Fig. 1). Investigating the TANN profile, Schuster et al. (2024) inferred the Middle Pleistocene evolution of the Tannwald Basin, a more than 200 m deep branch basin of the Rhine Glacier north of Lake Constance, as a prototype for this entire area: (i) erosion of Molasse bedrock at the bottom of the OD, more than 150 m below surface, by an advancing glacier, resulting in a glacial shear zone characterized by subglacial diamicts and bedrock fragments; (ii) sedimentation of fines in a proglacial lake with intermittent small-scale mass movements from basin slopes; (iii) progradation of more coarse-grained, sandy delta formations during continued glacial retreat; (iv) formation of a second inlaid basin by a successive glacial advance followed by deposition of laminated fines with diamictic interbeds; (v) continued glacial retreat and deposition of deltaic sand; and (vi) at the top, a last glacial advance with (glacio-)fluvial proglacial outwash consisting of gravels with interbedded diamicts in a now non-overdeepened setting. The authors stress that, although the investigated sediment sequences in the Tannwald Basin show three separate glacial advances, they do not all necessarily represent an independent glaciation but could represent shorter-term glacial fluctuations (Schuster et al., 2024). While the GAIS site appears to be situated in a more proximal part of the Tannwald Basin, drilling was initialized there to fill an Early to Middle Pleistocene stratigraphic gap based on the assumption that an older "Gaisbeuren Basin" may be located in this area, underlying the southern part of the Tannwald Basin (LGRB, 2015).

2.2 Lichtenegg

The second site near Lichtenegg (LICH) lies on a ridge of Höchsten, a butte of pre-Quaternary bedrock forming the topographically highest point of the Lake Constance Amphitheatre at about 840 m a.s.l. From a few outcrops along the narrow Deggenhauser Valley (Fig. 1), glacial basin deposits are known to be buried beneath (presumably Early Pleistocene) glaciofluvial "Deckenschotter" (Fig. 1; Ellwanger et al., 2011; Penck and Brückner, 1909). Due to this exceptional stratigraphic position, these deposits are interpreted as potentially being the oldest preserved Pleistocene sediments in the amphitheater, and the LICH site is considered to be a bonus site of the ICDP DOVE project. It is one of only two known locations in the entire Rhine Glacier area where Deckenschotter units are enclosed between glacial sediments (Ellwanger et al., 2011; LGRB, 2015). The diamicts underlying the Deckenschotter accumulated into what is interpreted as the Lichtenegg Basin, a small OD basin formed by the Rhine Glacier during an Early Pleistocene stage (Bibus and Kösel, 2003; Rolf et al., 2012). Menzies and Ellwanger (2011) identified ample micromorphological evidence of subglacial soft-sediment deformation. This was recently supported by data from a second outcrop that suggest deposition of the upper part of the diamicts in an ice-advance context (Bamford et al., 2025).

3 Methods

3.1 Drillings

3.1.1 Gaisbeuren

The Gaisbeuren drilling (GAIS) was initialized by the Geological State Survey of Baden-Württemberg (LGRB), undertaken by BauGrund Süd GmbH, and incorporated into ICDP DOVE as core 5068_6_A. It was conducted in autumn 2016 some 3 km south of Bad Waldsee (location: 47.8880° N, 9.7113° E; ∼ 607 m a.s.l.; Fig. 1) and reached, after cutting through approx. 11 m of bedrock, a final depth of 144 m. To a depth of 62 m, percussion drilling was used, replaced further downward by a wireline coring system. The core material was collected in light- and air-proof liners with a diameter of about 100 mm and a length of 1 m. Approximately 14 % of the drill core was not recordable or got lost, mainly due to jammed cobbles or loss of circulation during the drilling, and sediment in underfilled liners may have sustained deformation during core handling. Water tables were encountered at fluctuating depths of about 8–23 m. Due to instability, the drill hole had to be telescoped several times with outer casing diameters from 419 to 146 mm.

3.1.2 Lichtenegg

The Lichtenegg (LICH) drilling, also initialized by LGRB and drilled by BauGrund Süd GmbH, is located on the northwestern side of the Höchsten butte (47.8345° N, 9.3764° E; ∼ 797 m a.s.l.; Fig. 1). In the preparation of the main well, a 79 m deep pilot hole was established in late 2015 with a down-the-hole drill to prospect the ground conditions. The main drilling (LICH) was conducted at a distance of about 10 m afterward, reaching the bedrock at approx. 63.7 m and terminating with a final depth of 76 m. The first 10 m of drilling was performed with percussion core drilling and, after encountering technical difficulties, the interval of 10–32 m was drilled destructively. At 32 m the approach was switched to wireline core drilling. Therefore, cuttings are only are available between 10 and 32 m; otherwise, the sediment was collected in liners with a core diameter of about 100 mm and a length of 1 m. Liners with partial core loss were already filled up with swelling clay at the drill site. No water tables were logged in the main well, but the pilot hole showed water at a depth of about 74 m that rose to 57 m the next day.

3.2 Geophysics

After the drillings were completed, the LIAG Institute for Applied Geophysics conducted in situ borehole geophysical measurements on both drill sites (Rolf and Wonik, 2021). We focus here on magnetic susceptibility and combined gamma logs; additional parameters are provided in the Supplement. At LICH, well loggings were done only on the pilot hole which had no casing. Therefore, the signal was only damped by the drill pipes (diameter: 178 mm outside, 160 mm inside), and the data are comparable over the whole section (Rolf and Wonik, 2021). At GAIS the drill pipes reached a depth of 120 m during the measurements and had an additional three outer casings (0–18.5, 18.5–36.5, and 36.5–62 m). The location of the pipe shoes is illustrated in Fig. 3 with blue triangles. In addition, magnetic susceptibility (partly with a Magnon logger at LIAG in Grubenhagen, partly with a GeoTek scanner at the German Federal Geological Survey BGR in Berlin) and natural remanent magnetization (with a cryogen magnetometer; Rolf, 2000, at LIAG in Grubenhagen) were measured on the cores in closed liners. Core sections with $\geq 2/3$ core loss are indicated as gaps in the litho-log in Figs. 3 and 4 due to the unclear position and state of bulk core material (see below). Regardless, some of those sections show geophysical data, as all available cores, including underfilled ones, were scanned.

3.3 Core handling, description, and analysis

3.3.1 Core related workflow

The approach of this study is based on a variety of experiences from recent studies into drill core records from overdeepened basins (e.g., Buechi et al., 2018, 2024; Gegg et al., 2025b; Dehnert et al., 2012; Schaller et al., 2023; Schuster et al., 2024; Schwenk et al., 2022a, b). The LICH cores were cut open directly after drilling and geophysical measurements, and one core half got sealed into plastic sheets for preservation, while GAIS cores remained unopened in the repository of LGRB until spring 2024. Then, in the preparation for cutting, underfilled core sections were filled up with swelling clay. The cores were then cut lengthwise into an archive, half of which was preserved and sealed. A working half was then used for further investigations and sampling. Both halves were wrapped in several layers of protective plastic film. As the LICH cores had been already opened in 2016, the unpreserved (working) half had dried out over the years, and, therefore, some sampling and analysis had to be performed on the sealed (archive) half as well. In the sedimentological documentation, we regard core sections filled with sediment to $\leq 1/3$ as gaps in recovery, because material in the underfilled liners is very prone to deformation, shifting and mixing, and therefore deemed unreliable.

3.3.2 Core analysis

After photographic documentation (LICH with a D-SLR camera, GAIS with a smartphone following Gegg and Gegg, 2023) each core meter was described sedimentologically. We examined prevalent grain sizes, type, thickness and contacts of layers, colors, secondary sediment structures, and core quality. Because large parts of our cores consist of diamictic sediments, we quantified their clast contents by visual comparison with a mafic color index chart as used in igneous petrology (Shvetsov, 1954). Based on this, we distinguish between diamictic fines (<10 % clasts), matrix-rich diamicts (10 %–30 % clasts), and clast-rich diamicts (>30 % clasts). In addition, we realized organic and carbonate content measurements with the loss-on-ignition (LOI) method after Heiri et al. (2001), executed according to the guidelines set by the International Organization for Standardization (2017) in ISO 14 142 688-2. Therefore, a small amount of sediment was heated to 550 °C in a furnace, resulting in the combustion of organic carbon C_{org}, whose content was determined from the sample's resultant mass loss LOI550 by multiplying with a factor of 0.5 (Vereş, 2002). As a subsequent step the samples were heated to a temperature of 950 °C, resulting in the calcination of carbonates and the release of CO_2. Granted that all carbonates appear to be $CaCO_3$, the content of carbonates can be assessed from the mass loss (LOI950) by multiplying it with the ratio of the molar weights of $CaCO_3$ and CO_2 ($=2.27$).

3.3.3 Lithotypes

The basis of our sedimentological analysis is the definition of recurring lithotypes (Fig. 2; Schaller et al., 2023; Schuster et al., 2024). In the ICDP 5068_6_A core (Fig. 3) we identified four sedimentological lithotypes on the basis of sedimentological descriptions and geophysical properties. The Lichtenegg drill core (Fig. 4) was divided into six lithotypes. The lithotypes are described in Fig. 2 combined with a representative core photo. A detailed description of both cores is added as a supplement to the paper. A commonality of all lithotypes is the low organic carbon content of ~ 1.5 %, while $CaCO_3$ contents are between 30 % and 50 %.

4 Results

4.1 Lithostratigraphic units

4.1.1 Gaisbeuren

The ICDP 5068_6_A core was divided into seven lithostratigraphic units, A–G (Fig. 3). The lowermost unit A contains 11 m of bedrock (133.0–144.0 m) that consists of strongly consolidated marl, silt and sandstone with variable, mottled coloration identified as Neogene Upper Freshwater Molasse (Buechi et al., 2024; Platt and Keller, 1992). The Quaternary base can be identified at 133.05 m depth by a sharp, subhorizontal contact between the Molasse and superposed diamictic deposits (Fig. 5a). Unit B shows moderately sorted diamictic fines (124.0–133.0 m) with a silty to sandy matrix where the $CaCO_3$ content is up to 45 %, which transitions into matrix-rich diamicts (117.0–124.0 m). The diamicts in this unit are strongly consolidated and distinctly deformed, including, in some sections, shear bands (Fig. 5b; Schwenk et al., 2022a). They also frequently contain faceted "flat-iron" clasts (Fig. 5c; Evans, 2018; Gomez et al., 2026; Menzies and Shilts, 2002). Unit C consists of massive, well-sorted, medium to coarse sands (106.0–117.0 m) containing some isolated outsized gravel clasts. The massive sands are interrupted by a matrix-rich diamict layer (109.0–110.0 m). Unit D is a large-scale fining-upward succession. It begins at the bottom with a matrix-supported diamict succession and with a silty to slightly sandy matrix with occasional occurrences of cobbles (80.4–106.0 m; see Fig. 5c). On top lies a variation from poorly to moderately sorted diamictic fines with increased carbonate content (65.0–80.4 m). Unit E displays a second package of consolidated matrix-rich diamicts (51.0–65.0 m) with deformation structures (Fig. 5d), some flat-iron clasts, and shear zones. In unit F massive diamictic fines (47.6–51.0 m) are overlain by a package of poorly sorted, matrix-supported, yellowish diamict (36.0–47.6 m). The yellowish diamict is matrix-rich with a silty to sandy matrix and is slightly gravelly and occasionally contains cobbles. In contrast, units B–E are of uniform beige-gray color. Unit F shows, at a depth of about 40 m, water escape structures across several meters in the shape of clastic dikes (Fig. 5e). Unit G is characterized by a notably higher clast content (Fig. 3), with frequent flat-iron shapes. It contains, at the bottom, a very poorly sorted, matrix-supported gray-yellow diamict (29.5–34.6 m), while the overlying poorly sorted, gray-yellow diamict has a silty to slightly sandy matrix. This predominantly matrix supported diamict (1.0–29.5 m) with gray-yellow to brown-gray colors shows, beginning at

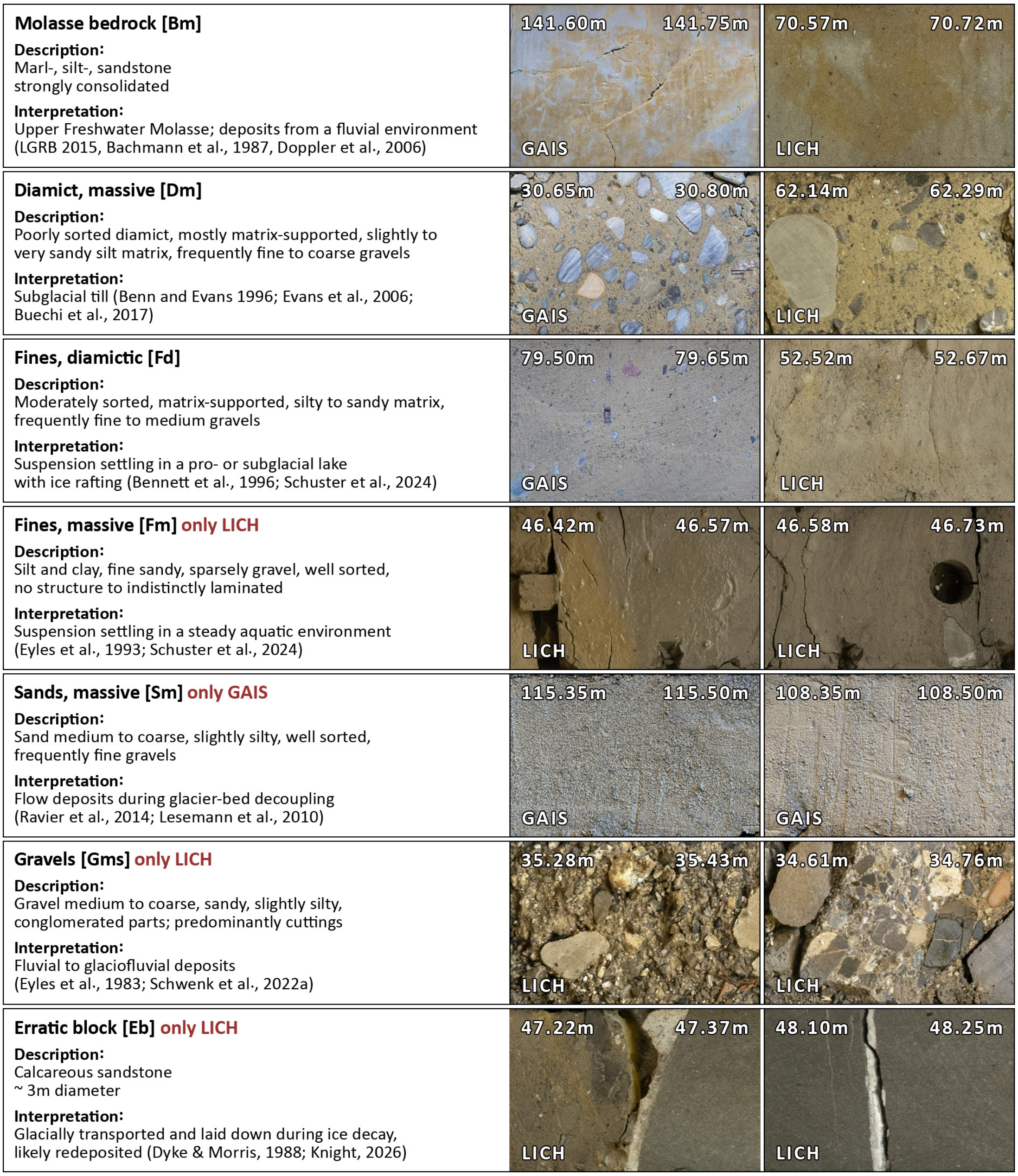

Figure 2. Lithotypes from both drill sites with description, general interpretation, and representative core photos (top is to the left). Note that some samples had been taken from the massive fines prior to photographing, and the resulting gaps are visible.

around 8 m depth, a fining-upward trend toward the topsoil (0.0–1.0 m).

4.1.2 Lichtenegg

The core LICH comprises five lithostratigraphic units (Fig. 4). The lowermost unit A contains 12 m of strongly consolidated marl, silt, and sand bedrock (63.7–75.6 m). The Quaternary base is located at 63.7 m depth with a sharp but irregular contact between the Molasse and the overlying diamictic fines (Fig. 5f). Unit B shows a fining-upward sequence of clast-rich diamicts, diamictic fines, and massive fines (44.4–63.7 m) overlying the Molasse bedrock, with shear zones, oriented clasts, and a decreasing number of gravel clasts. It is interrupted by a calcareous sandstone boulder with a diameter of ∼ 3 m. Following a diamict layer at 45.7–46.3 m, unit B terminates with a slightly fining-upward, poorly sorted but rather well-rounded gravel layer from 44.4 to 45.7 m. In contrast to other clast-rich intervals in LICH, flat-iron clasts are absent in this layer. It is

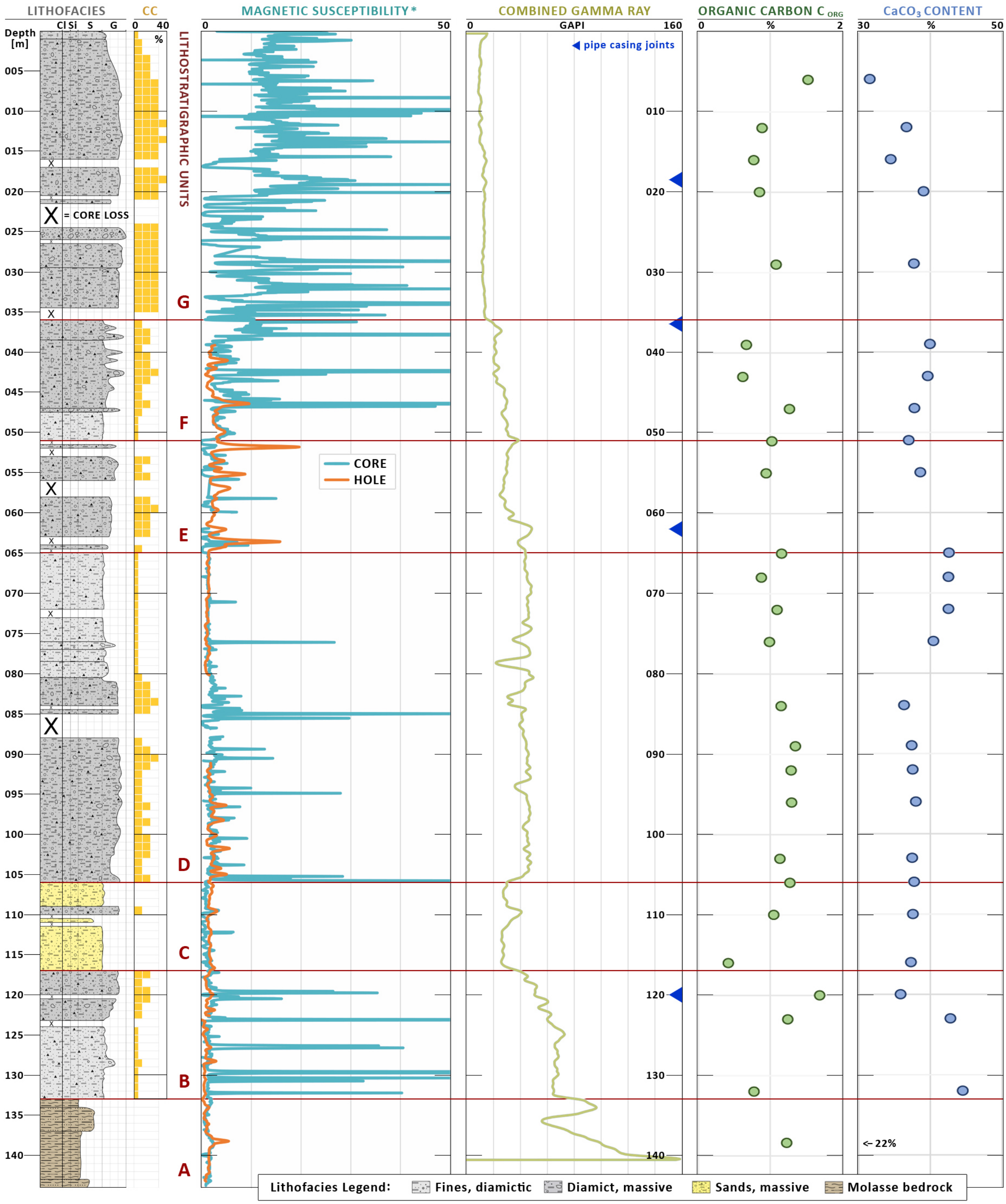

Figure 3. GAIS/5068_6_A composite plot: lithofacies log, CC (denoting clast content), lithostratigraphic units (separated by red lines), magnetic susceptibility (*logarithmic scale), combined gamma ray log from borehole, organic carbon content, and $CaCO_3$ content from loss-on-ignition analysis.

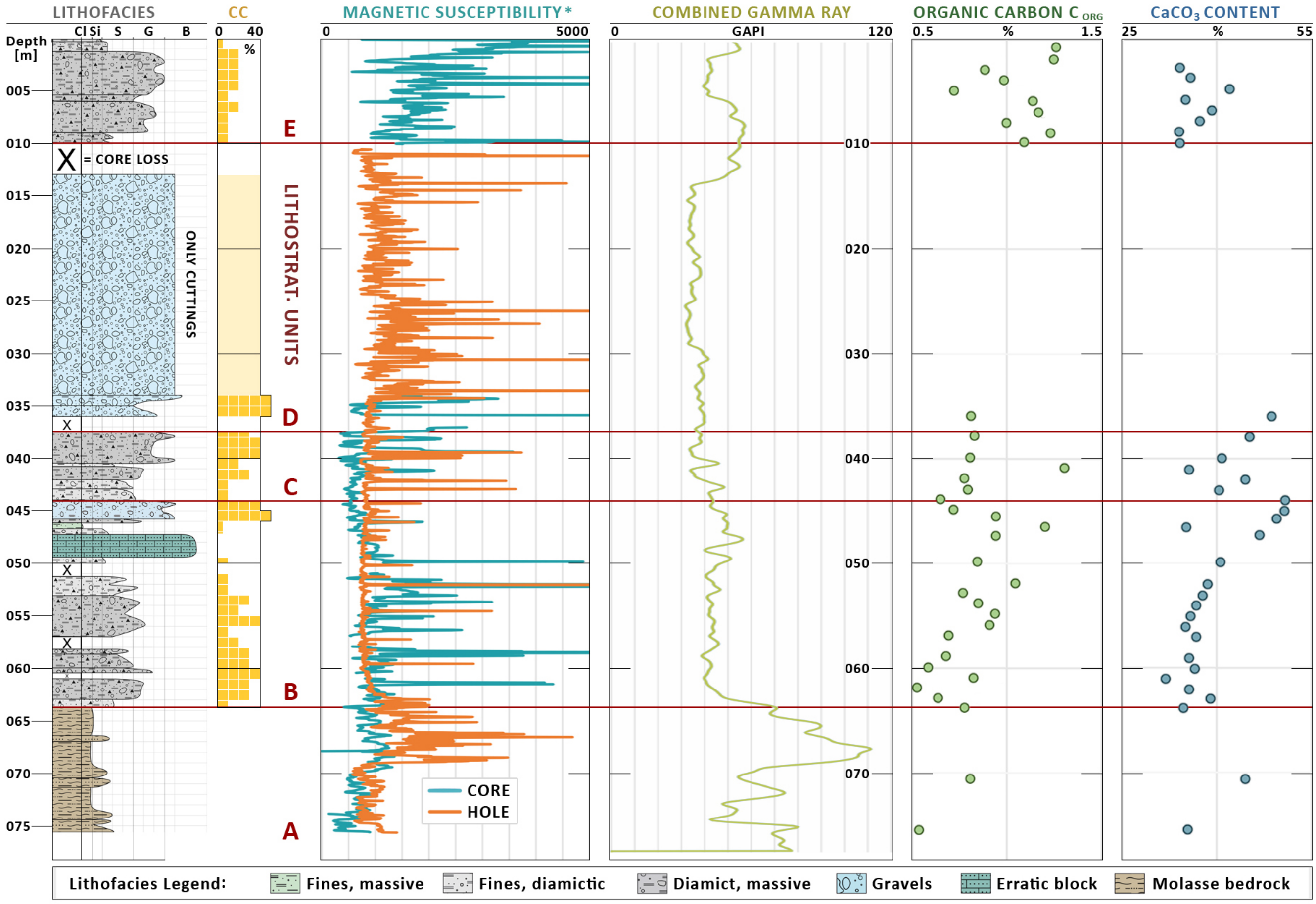

Figure 4. LICH composite plot: lithofacies log, CC (denoting clast content), lithostratigraphic units, magnetic susceptibility (*logarithmic scale), combined gamma ray log from pilot hole, organic carbon content, and $CaCO_3$ content from loss-on-ignition analysis.

noteworthy that both organic carbon and $CaCO_3$ content increase consistently throughout unit B, from ∼ 0.5 % to ∼ 1.2 % and from ∼ 35 % to ∼ 50 %, respectively. Unit C is a coarsening-upward sequence of diamictic fines and diamicts (37.7–44.4 m; Fig. 5g). Following a core-loss section, unit D consists of clast-supported, poorly sorted sandy gravels with conglomerated layers (10.0–36.0 m), of which only cuttings were available from 10 to 32 m. Unit E displays matrix supported and poorly sorted gray-brown diamicts (0.4–10.0 m) ending with a thin topsoil horizon (0.0–0.4 m). The interval from 5.0 to 5.4 m shows clasts with subhorizontal alignment and horizontal fractures (Fig. 5h).

4.2 Geophysics

Unit A from LICH shows, between 65 and 70 m depth, a distinct increase in magnetic susceptibility and combined gamma ray (up to > 100 GAPI) logs that both decrease again in the diamicts of unit B (see Fig. 4). The gamma log shows a slight increase over unit B from bottom to top and then decreases from unit C to D up to approx. 13 m depth. Between 5 and 13 m, the gamma signal is notably elevated at 50–60 GAPI. In unit E, magnetic susceptibility increases upward. Like in unit D, it has a significantly higher peak density than in unit B and C. GAIS core shows high magnetic susceptibility peak densities in units B, F, and G. The sandy Unit C in GAIS shows a clear drop of the combined gamma ray signal due to low clay content. Additional geophysical parameters are plotted in the appendix (Figs. A1 and A2 in the Appendix), and the original data are provided by Zeeden et al. (2026a, b).

5 Discussion

5.1 Genetic interpretation of the sediment successions

The classification of lithostratigraphic units in GAIS and LICH is mainly based on lithotypes with their particular sediment structures in correlation with geophysical characteristics, organic carbon, and carbonate content.

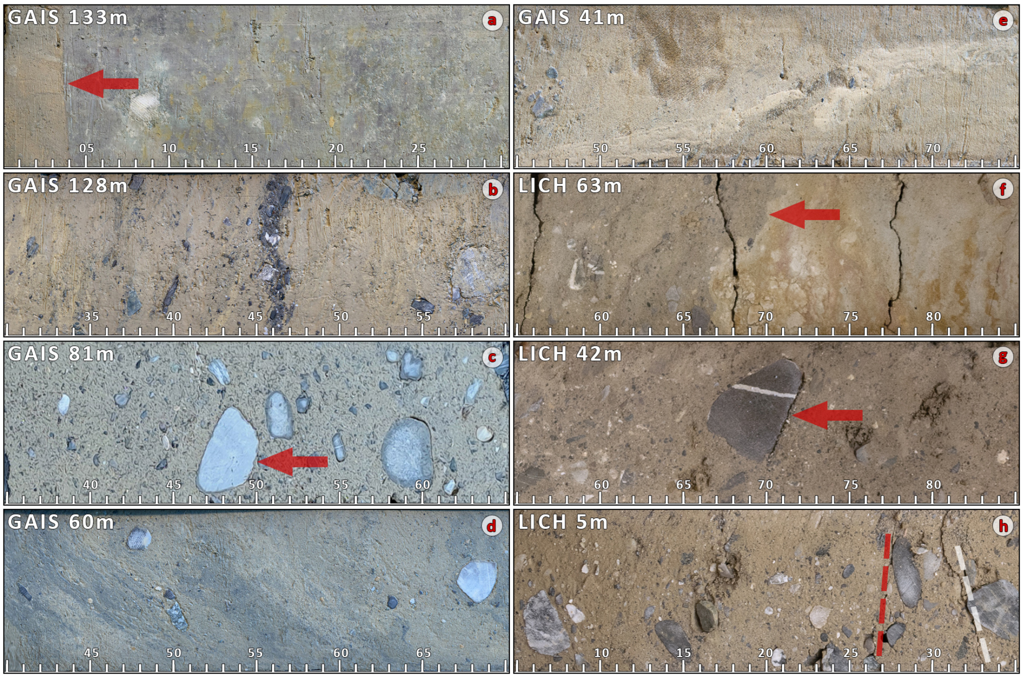

Figure 5. **(a–e)** Core sections from GAIS; **(a)** 133 m: sharp contact of basal till and Molasse bedrock (arrows); **(b)** 128 m: deformed diamict with shear band; **(c)** 81 m: flat-iron clasts (arrows; Evans, 2018; Menzies and Shilts, 2002) in diamict matrix; **(d)** 60 m: deformation structures in compact traction till; **(e)** 41 m: clastic dike (van der Meer et al., 2009; Ravier, 2024). **(f–h)** Core sections from LICH; **(f)** 63 m: sharp but irregular contact of basal till and Molasse bedrock (arrows); **(g)** 42 m: flat-iron clasts (arrows) in diamict matrix; **(h)** 5 m: horizontal alignment of clasts (red dashed) in sandy–silty matrix, likely by subglacial shearing. Dashed white: fracture.

5.1.1 Gaisbeuren

Unit A consists of Neogene Upper Freshwater Molasse bedrock, which had accumulated from Miocene Alpine rivers in an alluvial-plain setting (Bachmann et al., 1987; Doppler et al., 2006; LGRB, 2015). The overlying unit B is interpreted as subglacial traction till (Benn and Evans, 1996; Evans et al., 2006; Buechi et al., 2017) deposited at the sole of active, warm-based ice, with soft-sediment deformation structures (Fig. 5b) as evidence of glaciotectonic shearing. The genetic interpretation of the unstratified sands in unit C is less straightforward. They could be interpreted as ice-contact fan or deltaic deposits (Kessler et al., 2012; Schaller et al., 2023; Schwenk et al., 2022a), which would imply glacier retreat. In light of the overlying strata, however, we interpret the massive sands as subglacial channel fills from hyper-concentrated meltwater flows activated by glacial decoupling and lift-off (Lesemann et al., 2010; Ravier et al., 2014). We would expect such deposits to be somewhat stratified, but a drilling-related liquefaction of non-cohesive sand and, therefore, a disturbance of primary sediment structures is not unlikely (Gegg et al., 2025b). The thickest (41 m) unit, unit D, consists of a quite homogeneous fining-upward diamict succession, suggesting a relatively stable environment, which is supported by the very few changes in organic carbon and carbonate content and geophysical proxies. While it contains flat-iron clasts (Fig. 5c; Evans, 2018; Gomez et al., 2026; Menzies and Shilts, 2002) as indicators of ice proximity, there are no deformation structures, and we therefore interpret it as a melt-out till. It was likely deposited in a sub- to proglacial-lake setting (Bennett et al., 1996; Gegg et al., 2025b), and its fining-upward character indicates slightly decreasing glacial impact. Clear evidence of gravitational reworking, such as graded intervals, is missing. Unit E is specified as a second subglacial traction till due to its matrix showing, in some sections, persistent deformation structures (Fig. 5d), while other sections are entirely homogenized (Buechi et al., 2024; Evans et al., 2006; Schwenk et al., 2022a). The change from unit D to E is also underpinned by a distinct rise in magnetic susceptibility that points toward renewed coarse-grained sediment input into the basin, while the decline in the combined gamma ray signal is related to a change in pipe casing (blue triangles in Fig. 3). In addition, several smaller-scale gaps in recovery occur at the boundaries of and within unit E. This might relate to abrupt sediment mechanical changes, for example, in the state of consolidation or the cohesion of the sediment, which is to be expected in ice-contact deposits (and occurs also in other cores, e.g., in FA2 in Schwenk et al., 2022a; in unit A4 in Schaller et al., 2023; or in units 1–2 in Schuster et al., 2024). The overlying unit F is interpreted as a second melt-out till due to its mostly structureless sand-rich matrix (Evans et al., 2006). The clast-rich diamicts in unit G are assumed to be subglacial till in a now non-overdeepened setting. There, water can drain and transport fines away, resulting in the highest clast contents, high peak densities in magnetic susceptibility, and the lowest combined gamma ray signals of the core. Accordingly, the occurrence of clastic dikes (Fig. 5e) below indicates high water pressure gradients beneath the base of an overriding glacier (van der Meer et al., 2009; Ravier, 2024). Unit G appears, in general, to be a directionless structure but shows, in smaller sections, aligned clasts and deformation structures recurring over the unit (e.g., at 3 or 12–13 m depth). The section between 21 and 26 m is marked by core losses which could indicate another ice contact or simply a clast-richer zone in unit C.

5.1.2 Lichtenegg

Unit A consists of Upper Freshwater Molasse (Doppler et al., 2006) bedrock, below the overdeepened Quaternary base. Unit B starts, at its bottom, with sheared and dense fine-grained basal traction tills (Evans et al., 2006; e.g., Fig. 5f) containing Molasse fragments and continues with structureless diamicts, likely melt-out tills, that transition into diamictic and, finally, well-sorted fines (Dehnert et al., 2012; Schuster et al., 2024; see also Eyles et al., 1993). This succession corresponds to an initially active and erosive glacier that slowly decays and eventually vanishes from the basin. The pierced boulder at ∼ 48 m depth is of Alpine provenance and has clearly been transported toward the drill site by a glacier (Dyke and Morris, 1988; Knight, 2026; Veness et al., 2025). However, its position in the upper section of Unit B, on top of well-sorted fines, speaks against a primary deposition from melting ice. We suggest that it was redeposited here, for example, by a mass movement from a nearby moraine (Knight, 2026). The top of Unit B consists of a moderately well-sorted gravel layer with rounded clasts, indicating fluvial transport and, therefore, a deltaic or non-overdeepened setting (Dehnert et al., 2012; Gegg et al., 2025b; Schwenk et al., 2022a). Unit B shows a clear, constant increase in carbonate content, indicating a decreasing contribution from reworked Molasse bedrock and more far-transported material from the calcareous Alps. Organic carbon content increases in parallel, which may be due to decreasing sedimentation rates and, therefore, reduced dilution of organic material imported into the basin or, possibly, a slight warming trend. Altogether, these developments indicate an initial ice-retreat phase. Unit C, in contrast, marks a second phase of active glacial deposition and, therefore, an ice-advance scenario. This is represented by diamict layers containing distinct flat-iron clasts and aligned clasts (Fig. 5g), concomitant with a considerable drop in organic carbon. Unit D, with more than 25 m of partly cemented gravels was, deposited by meltwater streams (Dehnert et al., 2012; Schwenk et al., 2022a; see also Eyles et al., 1983). Because these gravels are, for the most part, only available as cuttings, we cannot draw more detailed conclusions regarding the depositional setting or further subdivisions. The uppermost unit E consists of till deposits with, in some intervals, a pronounced sub-horizontal clast fabric and sub-horizontal fractures (Fig. 5h), fitting to subglacial traction and lodgement (Evans, 2018; Hooyer and Iverson, 2000).

5.2 Implications for the depositional setting

Gegg and Preusser (2023) summarized OD structures from drillings in the northern Alpine foreland and appointed typical OD fillings with diamicts and overlaying lacustrine sediments. These fining-upward successions reflect the transition from deposition in a subglacial to an ice-marginal and lastly ice-distal setting in a lake that develops in the overdeepened basin as soon as the ice begins to retreat. The two nearest ICDP DOVE cores, TANN (5068_1) and BASA (5068_2, Fig. 1), show the same patterns with diamictic, deltaic, and lacustrine successions (Schaller et al., 2023; Schuster et al., 2024) as previously investigated cores from nearby northern Switzerland (Buechi et al., 2018, 2024; Dehnert et al., 2012; Schlunegger et al., 2024; Schwenk et al., 2022a) and beyond (e.g., eastern Alpine foreland: Firla et al., 2024, 2026; Pomper et al., 2017). In contrast, the GAIS and LICH cores are clearly distinct as they show diamict-dominated successions. They frequently contain indicators of glacial origin such as flat-iron clasts (Evans, 2018, Fig. 5c and g), which leads to the general interpretation that the entirety of the diamict successions were deposited in a glacier-proximal position (Fig. 6). Considering the thickness of the successions, especially in GAIS, this indicates that the respective glacier front remained, with minor fluctuations only, in the vicinity of the drill site for a prolonged period of time or that the thick fillings resulted from exceptionally high deposition rates from a large sediment supply. Unfortunately, no seismic data are available from either site, and so we do not know the geometries of the diamictic deposits. However, we consider it to be possible that they are analogs of subaquatic moraines or moraine complexes that have been identified, for example, in Scotland (Bradwell and Stoker, 2023) and Ireland (Evans et al., 2012) but also in modern Alpine lakes in Switzerland such as Lake Thun (Fabbri et al., 2018) and Lake Lucerne (Hilbe et al., 2011). However, the GAIS and LICH cores show not only melt-out tills expected in subaquatic morainal successions but also distinct intervals of pervasive (sub-)glacial deformation. Those indicators of ice contact attest to periods of glacier advance and grounding and demonstrate that the investigated sequences are more complex than some known, more simple subaquatic moraines.

Bamford et al. (2025) document an outcrop of diamictic deposits at Lichtenegg (∼ 800 m from the LICH drill site) that they interpret as the infill of a smaller OD basin, which got eroded during the Early Pleistocene (see also Bibus and Kösel, 2003; Ellwanger et al., 2011; Rolf and Wonik, 2021). The sheared and overridden diamicts from the lower part of

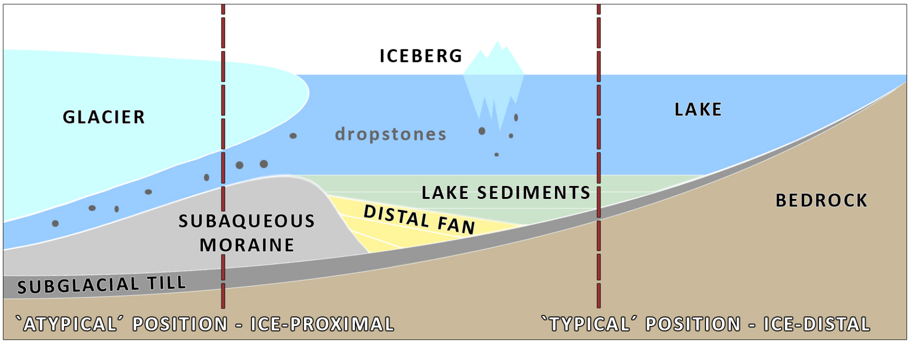

Figure 6. Schematic sketch of an overdeepening during ice retreat and infilling. Depending on the specific position, the sediment profile will either consist largely of lacustrine deposits ("typical" successions, shown on the right) or of diamictic-dominated deposits in the case of infilling in ice proximity (shown on the left).

the Lichtenegg outcrop were interpreted as secondary, i.e., slightly reworked glacial deposits, while the more massive and compact upper diamicts showed a primal glacial character. This corresponds to our interpretation regarding the transition from unit B to C in the LICH core, i.e., an ice-advance scenario. The gravels from LICH unit D therefore represent the Mindel–Deckenschotter; these represent the outcropping diamicts and were mapped extensively in this area (Bamford et al., 2025; LGRB, 2025). These are the youngest of a series of (glacio-)fluvial gravel units that are attributed to the Early Pleistocene (Ellwanger et al., 2011). The Deckenschotter is overlain by diamicts at the Höchsten, as well as in the LICH core, and those tills are classified as deposits from later cold phases up to penultimate glaciation (LGRB, 2015).

The subglacial traction tills in units B and E from GAIS show a noticeable similarity with diamict layers from the TANN site ∼12 km to the north (Schuster et al., 2024). The succession at TANN is that of a "typical" overdeepening fill dominated by lacustrine sediments (see Sect. 2.1), which are underlain and interrupted by diamicts, which the authors interpreted as two separate ice advances. These diamicts occur in very similar stratigraphic positions and absolute elevations as the traction tills in GAIS (e.g., GAIS unit B at ∼550 m a.s.l. and the till within unit B of TANN at ∼530 m a.s.l.), and their potential correlation should be investigated in more detail.

6 Conclusions

ICDP DOVE and previous studies have investigated many ODs in the northern Alpine foreland. The typical sediment succession consists of glacial diamicts directly overlying the bedrock followed up by often monotonous, fine-grained basin fills. This is the sedimentary signature of glacial retreat; subglacial incision terminates and sediments are deposited first in an ice contact, then in a glaciolacustrine, and lastly in a pure lacustrine setting. Here, we introduced two new drill cores from ODs in the Lake Constance Amphitheatre, which are strikingly different because they show OD fills that begin with diamicts but continue all the way to the top of the basin fill with diamictic fines and diamict successions, only occasionally intercalated by massive fines and sands with no clear signs of stratification. We explain this by the position of the cores: while most previous drillings into OD infills were conducted at very distal sites that were probably only briefly reached by the respective glaciers, the investigated deposits are situated in a more proximal position. Here, glacier presence and deposition directly from ice seem to have been more prolonged, and the diamict successions might be analogues of subaquatic moraine successions, as identified in some Alpine lakes. In contrast to the rather simple structure of these subaquatic morainal deposits, the ice-contact sediments characterized here show periods of glacial advance and suggest a more complex depositional history. These findings further indicate that the typical OD sediment successions as described above are not necessarily representative of all OD fills but rather are representative of basin sections that were quickly abandoned through fast retreat of the respective glacier. This appears to apply primarily to their distal-most parts. Notably, in the case of the "atypical" GAIS profile, the TANN site some kilometers to the north could be the "typical", distal equivalent of the same basin fill, but their correlation is, for the moment, hypothetical only and still needs to be investigated in future studies.

Appendix A: Borehole – geophysical measurements

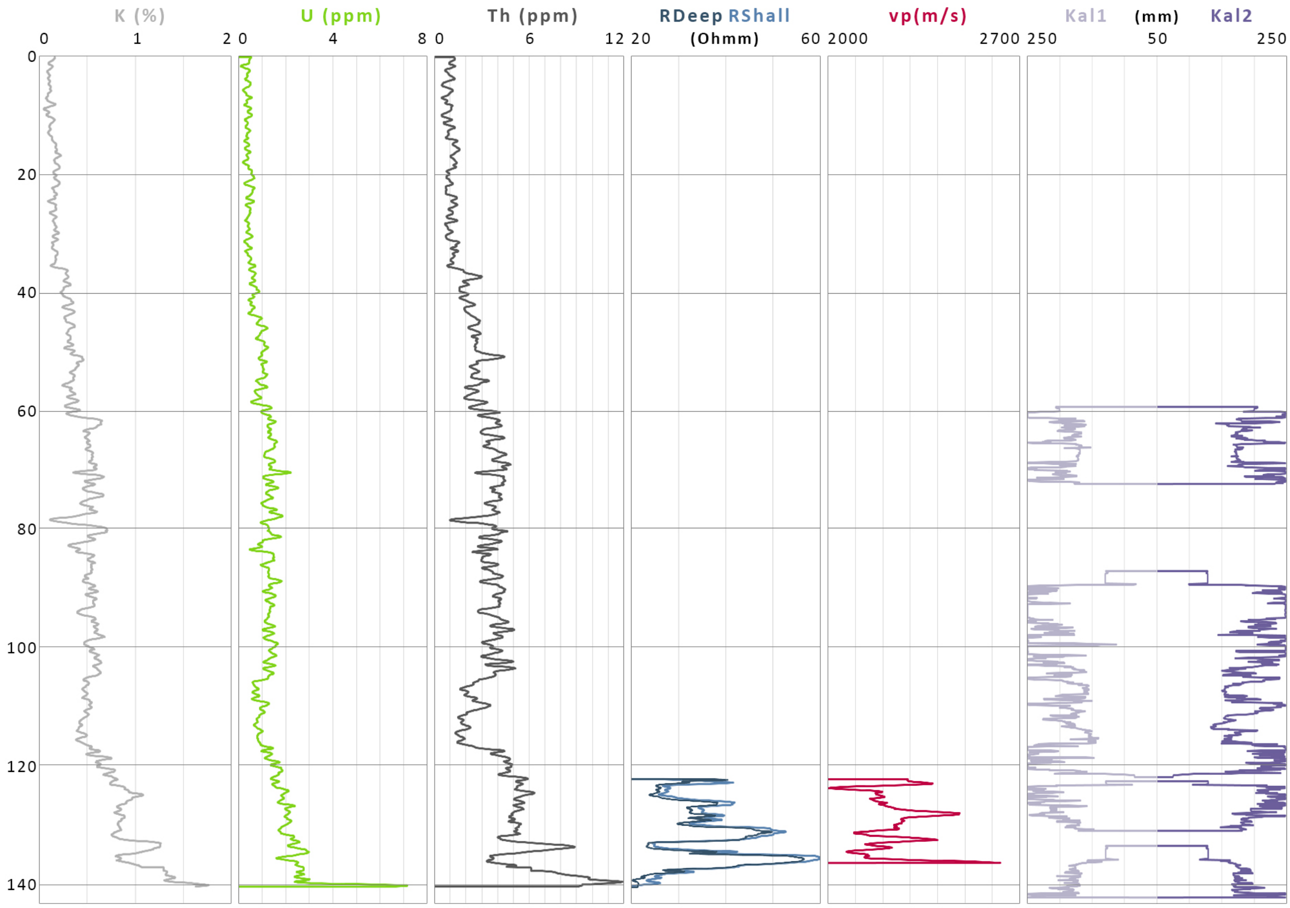

Figure A1. ICDP 5058_6 GAIS – composite plot: contents of potassium (K), uranium (U), and thorium (Th); RDeep/RShall: specific electrical resistance in two arrangements; vp: seismic P-wave velocities; Kal1/Kal2: borehole diameter (caliper log). The original data are provided by Zeeden et al. (2026a).

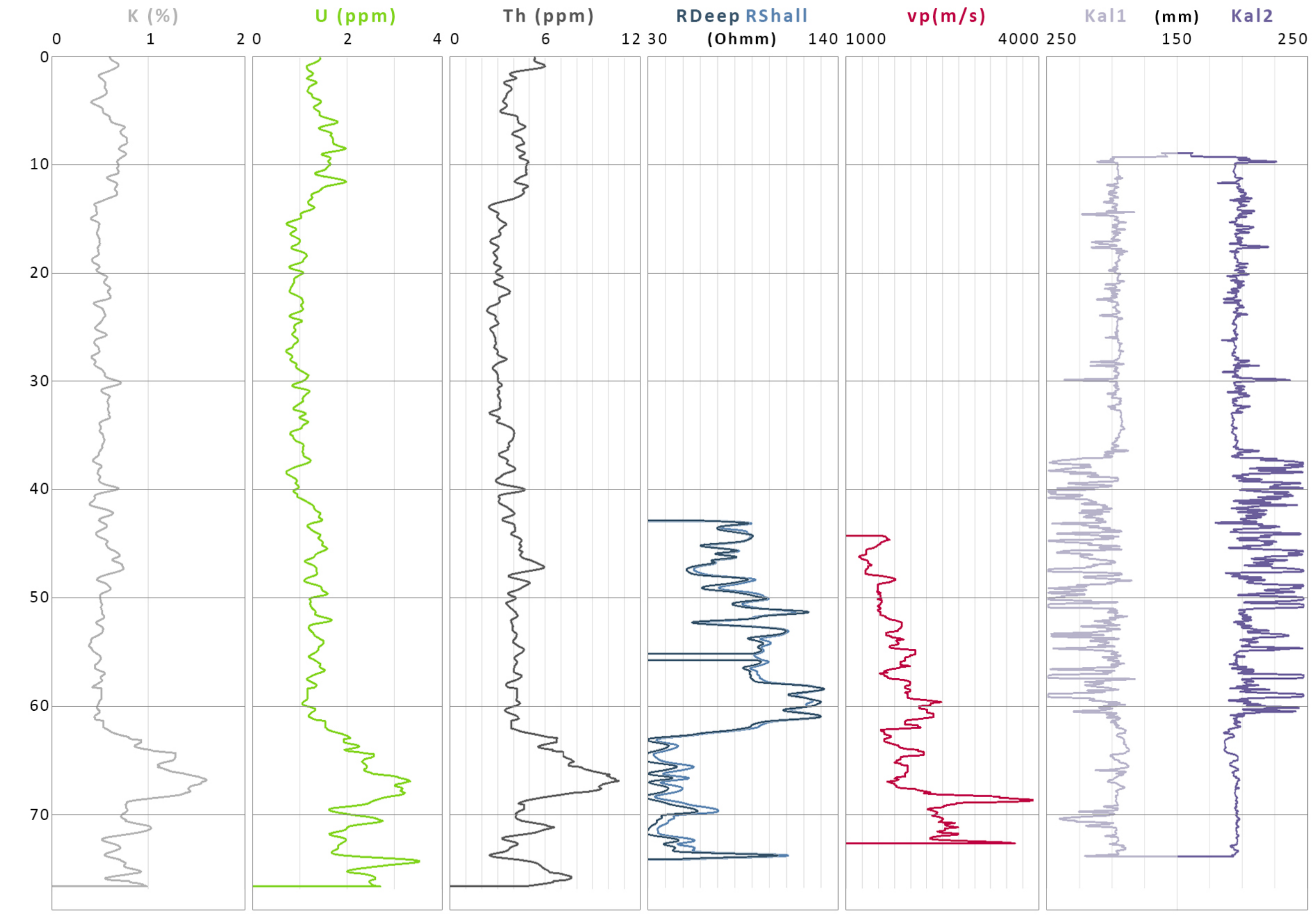

Figure A2. LICH – composite plot: contents of potassium (K), uranium (U), and thorium (Th); RDeep/RShall: specific electrical resistance in two arrangements; vp: seismic P-wave velocities; Kal1/Kal2: borehole diameter. The original data are provided by Zeeden et al. (2026b).

Data availability. The data that support our findings are provided in the Supplement and on the PANGAEA repository: https://doi.org/10.1594/PANGAEA.995767 (Zeeden et al., 2026a) and https://doi.org/10.1594/PANGAEA.995769 (Zeeden et al., 2026b).

Supplement. The supplement related to this article is available online at https://doi.org/10.5194/sd-35-193-2026-supplement.

Author contributions. JP: investigation, visualization, original draft preparation. LG: supervision, conceptualization, funding acquisition, investigation. FP: supervision, conceptualization. UWS provided resources and access to the cores, was the drill site executive geologist, and provided valuable insights into the geologic settings. CZ: data curation, methodology, validation. All of the authors approved the text and the figures and contributed to editing and validation.

Competing interests. The contact author has declared that none of the authors has any competing interests.

Disclaimer. Publisher's note: Copernicus Publications remains neutral with regard to jurisdictional claims made in the text, published maps, institutional affiliations, or any other geographical representation in this paper. The authors bear the ultimate responsibility for providing appropriate place names. Views expressed in the text are those of the authors and do not necessarily reflect the views of the publisher.

Acknowledgements. This publication is a contribution to the ICDP project DOVE. We would like to say a big thank you to Clare A. Bamford and Edwin Wambicho for their support with the core sampling and analysis in the core storage facility and the laboratory. A big shout-out is given to my office colleague F. Martin Hofmann for providing the working material and software data support. The Geological State Survey of Baden-Württemberg (LGRB Freiburg) supplied the drill cores, the records, and the workplace. Thanks are given to the LGRB Team from Unit 92, namely Melissa Gerlitzki, Stefan Gaß, and Frank Läufer, for the excellent collaboration in the core storage facility. Thanks are given to all of the DOVE Team members for the support and helpful discussions which improved this work, as well as to Fritz Schlunegger and an anonymous reviewer for the constructive recommendations. Expressions of gratitude are extended to Viktoria Moser for the constructive comments, interdisciplinary assistance, and patience during the writing of the paper.

The drilling operations GAIS and LICH were facilitated by the LGRB Freiburg.

Financial support. This research has been supported by the Deutsche Forschungsgemeinschaft (grant no. 517980590).

Review statement. This paper was edited by Nadine Hallmann and reviewed by Fritz Schlunegger and one anonymous referee.

References

Anselmetti, F. S., Bavec, M., Crouzet, C., Fiebig, M., Gabriel, G., Preusser, F., Ravazzi, C., and DOVE scientific team: Drilling Overdeepened Alpine Valleys (ICDP-DOVE): quantifying the age, extent, and environmental impact of Alpine glaciations, Sci. Dril., 31, 51–70, https://doi.org/10.5194/sd-31-51-2022, 2022.

Bachmann, G. H., Müller, M., and Weggen, K.: Evolution of the Molasse Basin (Germany, Switzerland), Tectonophysics, 137, 77–92, https://doi.org/10.1016/0040-1951(87)90315-5, 1987.

Bamford, C. A., Pomper, J. E., Hergarten, S., Preusser, F., Sprafke, T., and Gegg, L.: New insights into one of the oldest glacial deposits in the northern Alpine foreland (Höchsten, SW Germany), Boreas, 54, 729–743, https://doi.org/10.1111/bor.12684, 2025.

Bandou, D., Schlunegger, F., Kissling, E., Marti, U., Schwenk, M., Schläfli, P., Douillet, G., and Mair, D.: Three-dimensional gravity modelling of a Quaternary overdeepening fill in the Bern area of Switzerland discloses two stages of glacial carving, Sci. Rep., 12, 1441, https://doi.org/10.1038/s41598-022-04830-x, 2022.

Bandou, D., Schlunegger, F., Kissling, E., Marti, U., Reber, R., and Pfander, J.: Overdeepenings in the Swiss plateau: U-shaped geometries underlain by inner gorges, Swiss J. Geosci., 116, 19, https://doi.org/10.1186/s00015-023-00447-y, 2023.

Benn, D. I. and Evans, D. J. A.: The interpretation and classification of subglacially-deformed materials, Quat. Sci. Rev., 15, 23–52, https://doi.org/10.1016/0277-3791(95)00082-8, 1996.

Bennett, M. R., Doyle, P., and Mather, A. E.: Dropstones: their origin and significance, Palaeogeogr. Palaeoclimatol. Palaeoecol., 121, 331–339, https://doi.org/10.1016/0031-0182(95)00071-2, 1996.

Beraus, S., Burschil, T., Buness, H., Köhn, D., Bohlen, T., and Gabriel, G.: A comprehensive crosshole seismic experiment in glacial sediments at the ICDP DOVE site in the Tannwald Basin, Sci. Dril., 33, 237–248, https://doi.org/10.5194/sd-33-237-2024, 2024.

Beraus, S., Köhn, D., Bohlen, T., Burschil, T., Schuster, B., Buness, H., and Gabriel, G.: Seismic crosshole full-waveform inversion of high-frequency SV-waves for glacial sediment characterization, Geophys. Prospect., 73, 1587–1605, https://doi.org/10.1111/1365-2478.70024, 2025.

Bibus, E. and Kösel, M.: Rezente und fossile Böden als Gliederungskriterium der Rheingletscherablagerungen am Höchsten, Z. Dtsch. Geol. Ges., 154, 343–356, https://doi.org/10.1127/zdgg/154/2003/343, 2003.

Bradwell, T. and Stoker, M.: Scottish Landform Example: subaqueous moraines around the Summer Isles and in the approaches to Loch Broom (Wester Ross Marine Protected Area), Scott. Geogr. J., 139, 20–36, https://doi.org/10.1080/14702541.2023.2226452, 2023.

Buechi, M. W., Frank, S. M., Graf, H. R., Menzies, J., and Anselmetti, F. S.: Subglacial emplacement of tills and meltwater deposits at the base of overdeepened bedrock troughs, Sedimentology, 64, 658–685, https://doi.org/10.1111/sed.12319, 2017.

Buechi, M. W., Graf, H. R., Haldimann, P., Lowick, S. E., and Anselmetti, F. S.: Multiple Quaternary erosion and infill cycles in overdeepened basins of the northern Alpine foreland, Swiss J. Geosci., 111, 133–167, https://doi.org/10.1007/s00015-017-0289-9, 2018.

Buechi, M. W., Landgraf, A., Madritsch, H., Mueller, D., Knipping, M., Nyffenegger, F., Preusser, F., Schaller, S., Schnellmann, M., and Deplazes, G.: Terminal glacial overdeepenings: Patterns of erosion, infilling and new constraints on the glaciation history of Northern Switzerland, Quat. Sci. Rev., 344, 108970, https://doi.org/10.1016/j.quascirev.2024.108970, 2024.

Burschil, T., Buness, H., Tanner, D. C., Wielandt-Schuster, U., Ellwanger, D., and Gabriel, G.: High-resolution reflection seismics reveal the structure and the evolution of the Quaternary glacial Tannwald Basin, Surf. Geophys., 16, 593–610, https://doi.org/10.1002/nsg.12011, 2018.

Cohen, D., Jouvet, G., Zwinger, T., Landgraf, A., and Fischer, U. H.: Subglacial hydrology from high-resolution ice-flow simulations of the Rhine Glacier during the Last Glacial Maximum: a proxy for glacial erosion, E&G Quaternary Sci. J., 72, 189–201, https://doi.org/10.5194/egqsj-72-189-2023, 2023.

Cook, S. J. and Swift, D. A.: Subglacial basins: Their origin and importance in glacial systems and landscapes, Earth-Sci. Rev., 115, 332–372, https://doi.org/10.1016/j.earscirev.2012.09.009, 2012.

Dehnert, A., Lowick, S. E., Preusser, F., Anselmetti, F. S., Drescher-Schneider, R., Graf, H. R., Heller, F., Horstmeyer, H., Kemna, H. A., Nowaczyk, N. R., Züger, A., and Furrer, H.: Evolution of an overdeepened trough in the northern Alpine Foreland at Niederweningen, Switzerland, Quat. Sci. Rev., 34, 127–145, https://doi.org/10.1016/j.quascirev.2011.12.015, 2012.

Doppler, G., Heissig, K., and Reichenbacher, B.: Die Gliederung des Tertiars im suddeutschen Molassebecken, Newsl. Stratigr., 41, 359–375, https://doi.org/10.1127/0078-0421/2005/0041-0359, 2006.

Dürst Stucki, M. and Schlunegger, F.: Identification of erosional mechanisms during past glaciations based on a bedrock surface model of the central European Alps, Earth Planet. Sci. Lett., 384, 57–70, https://doi.org/10.1016/j.epsl.2013.10.009, 2013.

Dyke, A. S. and Morris, T. F.: Drumlin fields, dispersal trains, and ice streams in arctic Canada, Can. Geogr. Géographe Can., 32, 86–90, https://doi.org/10.1111/j.1541-0064.1988.tb00860.x, 1988.

Ellwanger, D., Wielandt-Schuster, U., Franz, M., and Simon, T.: The Quaternary of the southwest German Alpine

Foreland (Bodensee-Oberschwaben, Baden-Württemberg, Southwest Germany), E&G Quaternary Sci. J., 60, 22, https://doi.org/10.3285/eg.60.2-3.07, 2011.

Evans, D. J. A.: Till: A Glacial Process Sedimentology, Wiley-Blackwell, Chichester, 390 pp., https://doi.org/10.1002/9781118652541, 2018.

Evans, D. J. A., Phillips, E. R., Hiemstra, J. F., and Auton, C. A.: Subglacial till: Formation, sedimentary characteristics and classification, Earth-Sci. Rev., 78, 115–176, https://doi.org/10.1016/j.earscirev.2006.04.001, 2006.

Evans, D. J. A., Hiemstra, J. F., and Cofaigh, C. Ó.: Stratigraphic architecture and sedimentology of a Late Pleistocene subaqueous moraine complex, southwest Ireland, J. Quat. Sci., 27, 51–63, https://doi.org/10.1002/jqs.1513, 2012.

Eyles, C., Eyles, N., and França, A.: Glaciation and tectonics in an active intracratonic basin: the Late Palaeozoic Itararé Group, Paraná Basin, Brazil, Sedimentology, 40, 1–25, https://doi.org/10.1111/j.1365-3091.1993.tb01087.x, 1993.

Eyles, N., Eyles, C. H., and Miall, A. D.: Lithofacies types and vertical profile models; an alternative approach to the description and environmental interpretation of glacial diamict and diamictite sequences, Sedimentology, 30, 393–410, https://doi.org/10.1111/j.1365-3091.1983.tb00679.x, 1983.

Fabbri, S., Buechi, M. W., Horstmeyer, H., Hilbe, M., Hübscher, C., Schmelzbach, C., Weiss, B., and Anselmetti, F. S.: A subaquatic moraine complex in overdeepened Lake Thun (Switzerland) unravelling the deglaciation history of the Aare Glacier, Quat. Sci. Rev., 187, 62–79, https://doi.org/10.1016/j.quascirev.2018.03.010, 2018.

Fabbri, S. C., Haas, I., Kremer, K., Motta, D., Girardclos, S., and Anselmetti, F. S.: Subaqueous geomorphology and delta dynamics of Lake Brienz (Switzerland): implications for the sediment budget in the alpine realm, Swiss J. Geosci., 114, 22, https://doi.org/10.1186/s00015-021-00399-1, 2021.

Fiebig, M., Ellwanger, D., and Doppler, G.: Pleistocene glaciations of southern Germany, in: Developments in quaternary sciences, vol. 15, Elsevier, 163–173, https://doi.org/10.1016/B978-0-444-53447-7.00014-3, 2011.

Firla, G., Lüthgens, C., Neuhuber, S., Schmalfuss, C., Kroemer, E., Preusser, F., and Fiebig, M.: Analyzing complex single grain feldspar equivalent dose distributions for luminescence dating of glacially derived sediments, Quat. Geochronol., 85, 101627, https://doi.org/10.1016/j.quageo.2024.101627, 2024.

Firla, G., Lüthgens, C., Burschil, T., Neuhuber, S., Pini, R., Marchhart, O., Wieser, A., Schmalfuss, C., Kroemer, E., and Fiebig, M.: An MIS 8 terrestrial record retrieved from a glacially overdeepened basin in the northern foreland of the European Alps, E&G Quaternary Sci. J., 75, 85–105, https://doi.org/10.5194/egqsj-75-85-2026, 2026.

Gegg, L. and Gegg, J.: Poor Man's Line Scan – a simple tool for the acquisition of high-resolution, undistorted drill core photos, Sci. Dril., 32, 55–59, https://doi.org/10.5194/sd-32-55-2023, 2023.

Gegg, L. and Preusser, F.: Comparison of overdeepened structures in formerly glaciated areas of the northern Alpine foreland and northern central Europe, E&G Quaternary Sci. J., 72, 23–36, https://doi.org/10.5194/egqsj-72-23-2023, 2023.

Gegg, L., Deplazes, G., Keller, L., Madritsch, H., Spillmann, T., Anselmetti, F. S., and Buechi, M. W.: 3D morphology of a glacially overdeepened trough controlled by underlying bedrock geology, Geomorphology, 394, 107950, https://doi.org/10.1016/j.geomorph.2021.107950, 2021.

Gegg, L., Salcher, B. C., Pollhammer, T., Cohen, D., Fischer, U. H., and Landgraf, A.: An inventory of subglacial overdeepenings in southern Germany and Austria, Boreas, 54, 527–541, https://doi.org/10.1111/bor.12693, 2025a.

Gegg, L., Anselmetti, F. S., Deplazes, G., Fuelling, A., Madritsch, H., Mueller, D., Preusser, F., and Buechi, M. W.: Glaciations and landscape change in the Lower Aare Valley (Northern Switzerland) through the Middle Pleistocene, Quat. Res., 1–20, https://doi.org/10.1017/qua.2024.61, 2025b.

Gomez, N., Lowe, D., Mills, A., Slaney, N., and Arnott, R. W. C.: Ediacaran proximal glaciomarine sedimentation in the Bonavista Peninsula, Avalon Zone, Newfoundland, Canada, J. Sediment. Res., 96, 130–157, https://doi.org/10.2110/jsr.2025.022, 2026.

Heiri, O., Lotter, A. F., and Lemcke, G.: Loss on ignition as a method for estimating organic and carbonate content in sediments: reproducibility and comparability of results, J. Paleolimnol., 25, 101–110, https://doi.org/10.1023/A:1008119611481, 2001.

Hilbe, M., Anselmetti, F. S., Eilertsen, R. S., Hansen, L., and Wildi, W.: Subaqueous morphology of Lake Lucerne (Central Switzerland): implications for mass movements and glacial history, Swiss J. Geosci., 104, 425–443, https://doi.org/10.1007/s00015-011-0083-z, 2011.

Hooyer, T. S. and Iverson, N. R.: Clast-fabric development in a shearing granular material: Implications for subglacial till and fault gouge, Geol. Soc. Am. Bull., 112, 683–692, https://doi.org/10.1130/0016-7606(2000)112<683:CDIASG>2.0.CO;2, 2000.

International Organization for Standardization: Geotechnical investigation and testing – Identification and classification of soil Part 2: Principles for a classification, https://www.iso.org/standard/66346.html (last access: 13 August 2026), 2017.

Jong, M. G. G. D., Seyfried, H., Simon, T., Banzhaf, R., Schwab, A., Holuba, K.-H., and Müller, T.: The extent of the Rhine Glacier in eastern Upper Swabia (southern Germany) at the height of the Last Glacial Maximum: new morphological constraints from high-resolution digital terrain models, Z. Dtsch. Ges. Für Geowiss., 176, 795–823, https://doi.org/10.1127/zdgg/2025/0456, 2025.

Kamleitner, S., Ivy-Ochs, S., Manatschal, L., Akçar, N., Christl, M., Vockenhuber, C., Hajdas, I., and Synal, H.-A.: Last Glacial Maximum glacier fluctuations on the northern Alpine foreland: Geomorphological and chronological reconstructions from the Rhine and Reuss glacier systems, Geomorphology, 423, 108548, https://doi.org/10.1016/j.geomorph.2022.108548, 2023.

Kessler, T. C., Klint, K. E. S., Nilsson, B., and Bjerg, P. L.: Characterization of sand lenses embedded in tills, Quat. Sci. Rev., 53, 55–71, https://doi.org/10.1016/j.quascirev.2012.08.011, 2012.

Knight, J.: The interpretation of glacial erratics: late Pleistocene examples from Ireland, J. Palaeogeogr., 15, 100352, https://doi.org/10.1016/j.jop.2026.100352, 2026.

Lesemann, J.-E., Alsop, G. I., and Piotrowski, J. A.: Incremental subglacial meltwater sediment deposition and deformation associated with repeated ice-bed decoupling: a case study from the Island of Funen, Denmark, Quat. Sci. Rev., 29, 3212–3229, https://doi.org/10.1016/j.quascirev.2010.06.010, 2010.

LGRB: Lithostratigraphische Entwicklung des Baden-Württembergischen Rheingletschergebiets: Übertiefste Becken- und Moränen-Landschaft, LGRB-Fachbericht 2015/4, Freiburg i. Br., 86 pp., https://produkte.lgrb-bw.de/docPool/c525_data.pdf (last access: 13 August 2026), 2015.

LGRB: Geologische Karte von Baden-Wuerttemberg 1 : 50 000 (GeoLa), LGRB, https://maps.lgrb-bw.de/ (last access: 4 July 2025), 2025.

Menzies, J. and Ellwanger, D.: Insights into subglacial processes inferred from the micromorphological analyses of complex diamicton stratigraphy near Illmensee-Lichtenegg, Höchsten, Germany, Boreas, 40, 271–288, https://doi.org/10.1111/j.1502-3885.2010.00194.x, 2011.

Menzies, J. and Shilts, B. W.: 8 – Subglacial environments, in: Modern and Past Glacial Environments, edited by: Menzies, J., Butterworth-Heinemann, Oxford, 183–278, https://doi.org/10.1016/B978-075064226-2/50011-8, 2002.

Monegato, G. and Ravazzi, C.: The late pleistocene multifold glaciation in the alps: updates and open questions, Alp. Mediterr. Quat., 31, 225–229, https://doi.org/10.26382/AIQUA.2018.AIQUAconference, 2018.

Monegato, G., Gianotti, F., Ivy-Ochs, S., Reitner, J. M., Scardia, G., and Akçar, N.: The Early and Middle Pleistocene Glaciations in the Alps, Alp. Mediterr. Quat., 36, 127–148, https://doi.org/10.26382/AMQ.2023.07, 2023.

Penck, A. and Brückner, E.: Die Alpen im Eiszeitalter, Chr. Herm. Tauchnitz, Leipzig, 1909.

Platt, N. H. and Keller, B.: Distal alluvial deposits in a foreland basin setting – the Lower Freshwater Miocene), Switzerland: sedimentology, architecture and palaeosols, Sedimentology, 39, 545–565, https://doi.org/10.1111/j.1365-3091.1992.tb02136.x, 1992.

Pomper, J., Salcher, B. C., Eichkitz, C., Prasicek, G., Lang, A., Lindner, M., and Götz, J.: The glacially overdeepened trough of the Salzach Valley, Austria: Bedrock geometry and sedimentary fill of a major Alpine subglacial basin, Geomorphology, 295, 147–158, https://doi.org/10.1016/j.geomorph.2017.07.009, 2017.

Preusser, F., Graf, H. R., Keller, O., Krayss, E., and Schlüchter, C.: Quaternary glaciation history of northern Switzerland, E&G Quaternary Sci. J., 60, 21, https://doi.org/10.3285/eg.60.2-3.06, 2011.

Ravier, E.: Physical characteristics of hydrofracture systems and their fills in glacial sediments, Sediment. Geol., 463, 106593, https://doi.org/10.1016/j.sedgeo.2024.106593, 2024.

Ravier, E., Buoncristiani, J.-F., Clerc, S., Guiraud, M., Menzies, J., and Portier, E.: Sedimentological and deformational criteria for discriminating subglaciofluvial deposits from subaqueous ice-contact fan deposits: A Pleistocene example (Ireland), Sedimentology, 61, 1382–1410, https://doi.org/10.1111/sed.12111, 2014.

Rolf, C.: Das Kryogenmagnetometer im Magnetiklabor Grubenhagen, Geol. Jahrb., 52, 161–188, 2000.

Rolf, C. and Wonik, T.: Die Forschungsbohrungen Lichtenegg und Gaisbeuren (Baden-Württemberg): Gesteinsmagnetik und Bohrlochgeophysik, Leibnitz Institut für Angewandte Geophysik, Hannover, 2021.

Rolf, C., Fromm, K., and Ellwanger, D.: Zur Magnetostratigraphie an Deckenschottern aus dem südlichen Oberschwaben, LGRB Informationen, 26, 171–180, 2012.

Schaller, S., Buechi, M. W., Schuster, B., and Anselmetti, F. S.: Drilling into a deep buried valley (ICDP DOVE): a 252 m long sediment succession from a glacial overdeepening in northwestern Switzerland, Sci. Dril., 32, 27–42, https://doi.org/10.5194/sd-32-27-2023, 2023.

Schaller, S., Becerra, P., Beraus, S., Buechi, M. W., Mair, D., Sardar Abadi, M., Schuster, B., and Anselmetti, F. S.: Data-driven lithofacies prediction of unconsolidated sediments from wireline logs, Sedimentologika, 3, 1–18, https://doi.org/10.57035/journals/sdk.2025.e31.1819, 2025.

Schlunegger, F., Kissling, E., Bandou, D. T., Douillet, G. A., Mair, D., Marti, U., Reber, R., Schläfli, P., and Schwenk, M. A.: The Aare main overdeepening on the northern margin of the European Alps: basins, riegels, and slot canyons, Earth Surf. Dynam., 12, 1371–1389, https://doi.org/10.5194/esurf-12-1371-2024, 2024.

Schmalfuss, C., Neuhuber, S., Firla, G., Lüthgens, C., Schuster, B., Gegg, L., Anselmetti, F. S., and Fiebig, M.: Revisiting the "Hole of Bad Aussee": A key sedimentary record of Quaternary landscape dynamics in the Eastern Alps (Austria), Quat. Int., 755, 110086, https://doi.org/10.1016/j.quaint.2025.110086, 2026.

Schuster, B., Gegg, L., Schaller, S., Buechi, M. W., Tanner, D. C., Wielandt-Schuster, U., Anselmetti, F. S., and Preusser, F.: Shaped and filled by the Rhine Glacier: the overdeepened Tannwald Basin in southwestern Germany, Sci. Dril., 33, 191–206, https://doi.org/10.5194/sd-33-191-2024, 2024.

Schwenk, M. A., Schläfli, P., Bandou, D., Gribenski, N., Douillet, G. A., and Schlunegger, F.: From glacial erosion to basin overfill: a 240 m-thick overdeepening–fill sequence in Bern, Switzerland, Sci. Dril., 30, 17–42, https://doi.org/10.5194/sd-30-17-2022, 2022a.

Schwenk, M. A., Stutenbecker, L., Schläfli, P., Bandou, D., and Schlunegger, F.: Two glaciers and one sedimentary sink: the competing role of the Aare and the Valais glaciers in filling an overdeepened trough inferred from provenance analysis, E&G Quaternary Sci. J., 71, 163–190, https://doi.org/10.5194/egqsj-71-163-2022, 2022b.

Shvetsov, M.: Concerning Some Additional Aids in Studying Sedimentary Formations, Bull. Mosc. Soc. Nat., 29, 61–66, 1954.

Swisstopo 2025: Federal Office of Topography, swissBEDROCK 1 : 25 000 (TopFels25), https://www.swisstopo.admin.ch/en/3d-swissbedrock-en, last access: 10 December 2025.

Tomonaga, Y., Buechi, M. W., Deplazes, G., and Kipfer, R.: First dating of an early Chibanian (Middle Pleistocene) glacial overdeepening in the Alpine Foreland using the 4He/U-Th method, Geology, 53, 40–44, https://doi.org/10.1130/G52544.1, 2024.

van der Meer, J. J. M., Kjær, K. H., Krüger, J., Rabassa, J., and Kilfeather, A. A.: Under pressure: clastic dykes in glacial settings, Quat. Sci. Rev., 28, 708–720, https://doi.org/10.1016/j.quascirev.2008.07.017, 2009.

Veness, R. L., Clark, C. D., Ely, J. C., Knight, J. L., Igneczi, A., and Bradley, S. L.: Modelling erratic dispersal accounting for shifting ice flow geometries: A new method and explanations of erratic dispersal of the British–Irish Ice Sheet, J. Quat. Sci., 40, 944–957, https://doi.org/10.1002/jqs.3720, 2025.

Vereş, D. Ş.: A comparative study between loss on ignition and total carbon analysis on Mineralogenic sediments, Stud. UBB Geol., 47, 171–182, 2002.

Zeeden, C., Ulfers, A., Wonik, T., and Grelle, T.: Downhole logging data from DOVE-ICDP borehole 5068_6 at Gaisbeuren, PANGAEA [data set], https://doi.org/10.1594/PANGAEA.995767, 2026a.

Zeeden, C., Ulfers, A., Wonik, T., and Grelle, T.: Downhole logging data from DOVE-ICDP borehole 5068_H at Lichtenegg, PANGAEA [data set], https://doi.org/10.1594/PANGAEA.995769, 2026b.